

Naval Research Laboratory

Washington, DC 20375-5320



NRL/MR/6750--07-9030

Hamiltonian Analysis of Charged Particle Gyromotion in Cylindrical Coordinates

WILLIAM E. AMATUCCI

PETER W. SCHUCK

GURUDAS GANGULI

Charged Particle Physics Branch

Plasma Physics Division

DAVID N. WALKER

SFA, Inc.

Crofton, MD

April 27, 2007

Approved for public release; distribution is unlimited.

REPORT DOCUMENTATION PAGE

*Form Approved
OMB No. 0704-0188*

Public reporting burden for this collection of information is estimated to average 1 hour per response, including the time for reviewing instructions, searching existing data sources, gathering and maintaining the data needed, and completing and reviewing this collection of information. Send comments regarding this burden estimate or any other aspect of this collection of information, including suggestions for reducing this burden to Department of Defense, Washington Headquarters Services, Directorate for Information Operations and Reports (0704-0188), 1215 Jefferson Davis Highway, Suite 1204, Arlington, VA 22202-4302. Respondents should be aware that notwithstanding any other provision of law, no person shall be subject to any penalty for failing to comply with a collection of information if it does not display a currently valid OMB control number. **PLEASE DO NOT RETURN YOUR FORM TO THE ABOVE ADDRESS.**

1. REPORT DATE (DD-MM-YYYY) 27-04-2007			2. REPORT TYPE Memorandum Report		3. DATES COVERED (From - To)	
4. TITLE AND SUBTITLE Hamiltonian Analysis of Charged Particle Gyromotion in Cylindrical Coordinates					5a. CONTRACT NUMBER	
					5b. GRANT NUMBER	
					5c. PROGRAM ELEMENT NUMBER	
6. AUTHOR(S) William E. Amatucci, Peter W. Schuck, Gurudas Ganguli, and David N. Walker*					5d. PROJECT NUMBER 67-3419-17	
					5e. TASK NUMBER	
					5f. WORK UNIT NUMBER	
7. PERFORMING ORGANIZATION NAME(S) AND ADDRESS(ES) Naval Research Laboratory 4555 Overlook Avenue, SW Washington, DC 20375-5320					8. PERFORMING ORGANIZATION REPORT NUMBER NRL/MR/6750--07-9030	
9. SPONSORING / MONITORING AGENCY NAME(S) AND ADDRESS(ES) Office of Naval Research One Liberty Center 875 North Randolph Street, Suite 1425 Arlington, VA 22203					10. SPONSOR / MONITOR'S ACRONYM(S) ONR	11. SPONSOR / MONITOR'S REPORT NUMBER(S)
12. DISTRIBUTION / AVAILABILITY STATEMENT Approved for public release; distribution is unlimited.						
13. SUPPLEMENTARY NOTES *SFA, Inc., Crofton, MD 21114						
14. ABSTRACT A Hamiltonian approach in cylindrical coordinates is applied to the motion of charged particles in a uniform axial magnetic field. The method is compared to the traditional approaches of uniform circular motion and Newtonian mechanics. Cylindrical coordinates are preferred in many practical situations such as application to laboratory experiments. The advantage cylindrical coordinates offer is the ability to form a one-dimensional effective potential, which can be used to determine a number of spatial and temporal characteristics of the resulting cyclotron motion without an explicit solution of the equations of motion. This approach provides a different perspective into the dynamics of Larmor motion to complement the traditional approaches.						
15. SUBJECT TERMS Cyclotron motion Hamiltonian dynamics						
16. SECURITY CLASSIFICATION OF:			17. LIMITATION OF ABSTRACT UL	18. NUMBER OF PAGES 24	19a. NAME OF RESPONSIBLE PERSON William E. Amatucci	
a. REPORT Unclassified	b. ABSTRACT Unclassified	c. THIS PAGE Unclassified			19b. TELEPHONE NUMBER (include area code) (202) 404-1022	

Hamiltonian analysis of charged particle gyromotion in cylindrical coordinates

W. E. Amatucci, P. W. Schuck, and G. Ganguli

Plasma Physics Division, Naval Research Laboratory, Washington, DC 20375

D. N. Walker

SFA, Inc., Crofton, MD 21114

A Hamiltonian approach in cylindrical coordinates is applied to the motion of charged particles in a uniform axial magnetic field. The method is compared to the traditional approaches of uniform circular motion and Newtonian mechanics. Cylindrical coordinates are preferred in many practical situations such as application to laboratory experiments. The advantage cylindrical coordinates offer is the ability to form a one-dimensional effective potential, which can be used to determine a number of spatial and temporal characteristics of the resulting cyclotron motion without an explicit solution of the equations of motion. This approach provides a different perspective into the dynamics of Larmor motion to compliment the traditional approaches.

PACS: 01.55.+b, 45.20.Jj, 51.60.+a, 52.20.Dq, 52.65.Cc

I. INTRODUCTION

The force acting on moving charges in a magnetic field and the resulting cyclotron motion are familiar concepts to students. In undergraduate introductory

Manuscript approved February 20, 2007.

physics courses, the magnetic force is introduced along with the electric force in a description of the Lorentz force, $\vec{F} = q\vec{E} + q\vec{v} \times \vec{B}$, which shows that the magnetic force acts at right angles to both the magnetic field and the velocity vector. Here, \vec{F} is the force, q is the particle charge, \vec{v} is the particle velocity, and \vec{E} and \vec{B} are the electric and magnetic fields. At the introductory level, by setting $E = 0$, cyclotron motion is often introduced with a uniform circular motion treatment.¹ By equating the magnetic force qvB to the centripetal force $\frac{mv^2}{r}$, one can quickly solve for r and define it to be the particle gyroradius $\rho \equiv \frac{mv}{qB}$. The angular velocity is then defined as the particle cyclotron frequency, which is given by the relation $\Omega \equiv \frac{\nu}{\rho} = \frac{qB}{m}$. Effectively, this treats the motion in cylindrical coordinates, placing the origin of the coordinate system at the center of the particle gyro orbit.

In later courses, such as undergraduate level introductory plasma physics courses, cyclotron motion is frequently described by single-particle motion in a plasma by application of Newton's 2nd Law,² $m \frac{d\vec{v}}{dt} = q\vec{v} \times \vec{B}$ in Cartesian coordinates. With uniform magnetic field taken in the \hat{z} direction, the components of this equation yield the coupled differential equations

$$m \frac{dv_x}{dt} = qBv_y \quad \text{and} \quad m \frac{dv_y}{dt} = -qBv_x.$$

Differentiating each with respect to time and substituting, we have a description of simple harmonic motion at the cyclotron frequency,

$$\frac{d^2v_x}{dt^2} = -\left(\frac{qB}{m}\right)^2 v_x = -\Omega^2 v_x \quad \text{and} \quad \frac{d^2v_y}{dt^2} = -\left(\frac{qB}{m}\right)^2 v_y = -\Omega^2 v_y.$$

One advantage of this treatment in Cartesian coordinates over the earlier uniform circular motion treatment is that the particle orbit does not have to be centered on the origin. This is a better description for practical applications in the sense that it yields uniform circular motion about some gyro center position that does not have to coincide with the origin of the coordinate system.

These approaches provide a basic foundation for understanding cyclotron motion and can be used as a starting point for analysis of more complicated motions, such as drifts superimposed on gyromotion in the presence of forces or gradients transverse to the magnetic field. The cross-magnetic-field drift motion of charged particles is important in space and laboratory plasmas, particularly when the drift is inhomogeneous. In such cases, nonuniformities in the cross-field flow can give rise to a variety of plasma instabilities,³ which in turn can cause particle heating and transport. However, in the analysis of particle dynamics in these realistic situations, the use of Cartesian coordinates can be awkward. For example, most laboratory plasma experiments are best described by cylindrical geometry.

As an initial step in a broader investigation of the dynamics of plasma ions in an experimental configuration containing an axial magnetic field, and a cylindrically symmetric, but radially inhomogeneous, electric field,⁴ we have performed a Hamiltonian

analysis in cylindrical coordinates of particle gyromotion in a uniform magnetic field. The intent is to develop solutions for particle orbits in the more experimentally convenient cylindrical geometry while allowing the center of the orbit to be located at arbitrary positions. While the Hamiltonian approach is equivalent to a Newtonian or Lagrangian analysis, it can provide some advantages. In cases where the multi-dimensional dynamics can be reduced to one dimension with an effective potential, much useful information regarding the orbit can be obtained, even if an explicit solution describing the orbit cannot. For example, a Hamiltonian treatment of charged particle motion in a magnetic mirror configuration with a radial electric field has been described by *Schmidt*.⁵

II. HAMILTONIAN APPROACH

The Lagrangian describing the motion of a charged particle in the presence of a time-independent magnetic field is given by

$$L = \frac{1}{2}mv^2 + q(\vec{A} \cdot \vec{v}), \quad (1)$$

where \vec{A} is the magnetic vector potential, and m , q , and \vec{v} are the particle mass, charge, and velocity, respectively. The Hamiltonian for the system is given by

$$H = \sum_i P_i \dot{Q}_i - L, \text{ where } \dot{Q}_i \text{ and } P_i \text{ are the time derivatives of the canonical coordinates}$$

and conjugate momenta, respectively. In cylindrical geometry with uniform axial magnetic field, the z coordinate can be ignored and only the 2-dimensional motion (r, θ)

of the particles need be considered. Under these conditions, the Lagrangian can be expressed in terms of the radial and azimuthal coordinates as

$$L = \frac{m}{2}(\dot{r}^2 + r^2\dot{\theta}^2) + qA_\theta r\dot{\theta}. \quad (2)$$

In cylindrical coordinates, the magnetic vector potential for a uniform axial magnetic field is $\vec{A} = \frac{rB_0}{2}\hat{\theta}$, which satisfies $\vec{B} = \vec{\nabla} \times \vec{A} = B_0\hat{z}$. Thus, the Lagrangian can be expressed as

$$L = \frac{m}{2}(\dot{r}^2 + r^2\dot{\theta}^2 + r^2\Omega\dot{\theta}). \quad (3)$$

Since the canonical momenta are defined as $P_i = \frac{\partial L}{\partial \dot{Q}_i}$, we have that

$$P_r = \frac{\partial L}{\partial \dot{r}} = m\dot{r} \Rightarrow \dot{r} = \frac{P_r}{m}, \text{ and that} \quad (4)$$

$$P_\theta = \frac{\partial L}{\partial \dot{\theta}} = mr^2\left(\dot{\theta} + \frac{\Omega}{2}\right) \Rightarrow \dot{\theta} = \frac{P_\theta}{mr^2} - \frac{\Omega}{2}. \quad (5)$$

Substituting these expressions into the Lagrangian, the Hamiltonian for the system becomes

$$H = \frac{P_r^2}{2m} + \frac{1}{2mr^2} \left(P_\theta - m\frac{\Omega}{2}r^2 \right)^2. \quad (6)$$

The time derivative of H is

$$\frac{dH}{dt} = \frac{\partial H}{\partial t} + \frac{\partial H}{\partial P_r} \dot{P}_r + \frac{\partial H}{\partial P_\theta} \dot{P}_\theta + \frac{\partial H}{\partial r} \dot{r} + \frac{\partial H}{\partial \theta} \dot{\theta}. \quad (7)$$

Using Hamilton's Equations, Equation 7 reduces to⁶

$$\frac{dH}{dt} = \frac{\partial H}{\partial t} + \dot{r}\dot{P}_r + \dot{\theta}\dot{P}_\theta - \dot{P}_r\dot{r} - \dot{P}_\theta\dot{\theta} = \frac{\partial H}{\partial t}. \quad (8)$$

Therefore, since the Hamiltonian does not depend explicitly on time, H is a constant of the motion and represents the total energy of the particle. Furthermore, since H does not explicitly depend on θ , $\dot{P}_\theta = -\frac{\partial H}{\partial \theta} = 0$, indicating that P_θ is also a constant of the motion.

This fact can be utilized by treating the second term on the right of Equation 6 as an effective potential

$$\psi(r) \equiv \frac{1}{2mr^2} \left(P_\theta - m\frac{\Omega}{2}r^2 \right)^2, \quad (9)$$

which constrains the motion of the charged particle. Therefore, the two-dimensional (r, θ) dynamics have been reduced to one dimension, r , with an effective potential $\psi(r)$. The usefulness of an effective potential in the analysis of charged particle orbits in magnetic fields has been described by *Stern*.⁷ Here, $\psi(r)$ describes a cylindrically symmetric potential well within which the particle motion is bound. Important orbital details such as the radial and azimuthal turning point positions, the orbital radius, and the gyroperiod

can be determined from $\psi(r)$, without an explicit solution to the radial and azimuthal equations of motion, $r(t)$ and $\theta(t)$.

The radial location of the minimum of the effective potential well determined from $\frac{\partial\psi}{\partial r} = 0$ is given by the equation

$$\frac{\partial\psi}{\partial r} = -\frac{1}{m} \left(\frac{P_\theta - m\frac{\Omega}{2}r^2}{r} \right) \left(\frac{P_\theta + m\frac{\Omega}{2}r^2}{r^2} \right) = 0. \quad (10)$$

Thus, two categories of solutions exist, Type I corresponding to $\left(P_\theta - m\frac{\Omega}{2}r^2 \right) = 0$ and

Type II corresponding to $\left(P_\theta + m\frac{\Omega}{2}r^2 \right) = 0$. Of course, in a uniform magnetic field,

identical circular orbits result for identical particles with the same initial velocity vector, independent of the initial radial position of the particle. However, even though the actual orbits are identical, the categories are distinguished by the effective potential, as determined by the initial position and velocity of the charged particle.

Type I orbits correspond to those which do not encompass the origin of the coordinate system. For this motion, the gyro orbit of the particle is entirely off-axis.

Solving $\left(P_\theta - m\frac{\Omega}{2}r^2 \right) = 0$ for r , we find that

$$r_m = \left(\frac{2P_\theta}{m\Omega} \right)^{\frac{1}{2}}, \quad (11)$$

which represents the radial position of the minimum of the effective potential. Here $P_\theta = mr^2 \left(\dot{\theta} + \frac{\Omega}{2} \right) = mr_0^2 \left(\dot{\theta}_0 + \frac{\Omega}{2} \right) = \text{constant}$, and r_0 and $\dot{\theta}_0$ are the initial values of the particle position and the angular velocity about the origin, respectively. One might anticipate that the minimum of the effective potential yields the position of the guiding center of the orbit. However, since the effective potential is not symmetric about the minimum, r_m does not, in general, give the guiding center of the gyromotion. (In contrast, the constants of integration in a Hamiltonian analysis in Cartesian coordinates do give the guiding center position, $x_{gc} = x_0 + \rho \sin \vartheta_0$ and $y_{gc} = y_0 - \rho \cos \vartheta_0$, where ϑ_0 is the initial angle of the velocity vector.) For Type I orbits, both the radial and azimuthal velocities change sign at points along the path since there are turning points in both the radial and azimuthal directions. By comparison with Equation 5, we see that the value of r_m gives the radius at the locations where $\dot{\theta} = 0$ (the azimuthal turning points). Since the velocity is purely radial at those two locations, another way of looking at r_m is that it is the radius of a circle centered on the origin that intersects the orbit normal to the particle trajectory.

In the radial direction, the turning points are determined from the solution of the equation $\psi(r) = \mathcal{E}_0$, where $\mathcal{E}_0 = \frac{1}{2}mv_0^2$ is the initial energy (and the total energy) of the particle. Therefore,

$$\frac{1}{2mr^2} \left(P_\theta - m \frac{\Omega}{2} r^2 \right)^2 = \frac{1}{2}mv_0^2, \quad (12)$$

which reduces to

$$r^4 - 2(r_m^2 + 2\rho^2)r^2 + r_m^4 = 0, \quad (13)$$

where $\rho \equiv \frac{v_0}{\Omega}$ is the particle gyroradius. The solution to the Equation 13 is

$$r_{TP+,-} = \left(r_m^2 + 2\rho^2 \right) \left[1 \pm \sqrt{1 - \left(1 + \frac{2\rho^2}{r_m^2} \right)^{-2}} \right]^{\frac{1}{2}}, \quad (14)$$

where r_{TP+} and r_{TP-} represent the outer and inner radial turning point positions, respectively. For Type I orbits, the two roots of this expression give the innermost and outermost radial position of the particle trajectory. Figure 1 shows a plot of the effective potential for a positively charged ion as a function of radius. The potential is normalized to the initial energy of the ion and the radial position is normalized to the ion gyroradius. For this plot, the initial position of the ion was chosen to be $r = 2.5\rho$ and the initial velocity was chosen to be at an angle of $-3\pi/4$ with respect to the horizontal (\hat{x}) direction. For these initial conditions, the entire orbit of the ion remains off axis. Since the azimuthal velocity goes to zero at distinct points in the orbit (when $r = r_m$), we see that the effective potential also goes to zero at $r = r_m$. Half of the separation distance between the two turning points, $(r_{TP+} - r_{TP-})/2 = \rho$, showing that the radius of the orbit is equal to the gyroradius as expected. The vertical black dashed-dotted line marks the radial location of the center of the orbit, r_{gc} , which is distinct from the radial position of the minimum in the potential. Figure 2 shows a schematic representation of an off-axis

ion gyro orbit, identifying the radial and azimuthal turning points, the gyroradius, and the guiding center position.

Figure 3 shows an intensity plot of the effective potential in the x - y plane with the ion gyro orbit corresponding to the initial conditions for Figure 1. For the intensity plot, black represents a value of 0, with white representing the largest magnitude of $\psi(r)$. The ion gyro orbit is indicated by the yellow line, which clearly does not encompass the origin. The inner and outer turning point radii are indicated by the white dashed circles and the circle with radius equal to r_m is shown as the red dashed line centered on the deepest part of the effective potential trough. From this plot, we can see that the inner and outer turning point radii define circles which are tangent to the particle gyro orbit.

Type II orbits correspond to those which do encompass the origin. Similar to Type I, the radial position of the effective potential minimum is $r_m = \left| \frac{2P_\theta}{m\Omega} \right|^{\frac{1}{2}}$. Unlike Type I, however, the angular velocity for Type II orbits never goes to zero. Consequently, while there is still a clear minimum in the potential, the value of $\psi(r_m)$ is never equal to zero for Type II orbits. Figure 4 is a plot of the effective potential for such a case. In this example, a positively charged ion is started from an initial radial position of 0.5ρ , again with the initial velocity at an angle of $-3\pi/4$ with respect to the \hat{x} direction. The magnetic field strength, ion mass, and initial velocity are the same as those for Figure 1, so the corresponding gyro orbits are the same size. Another distinguishing characteristic between Type I and Type II orbits is that the angular separation between the radial turning points for a Type I orbit is always 0 while for Type II orbits the angular separation is equal to π . Thus, in this example, since the inner and

outer radial turning points occur on ‘opposite sides’ of the origin, their separation is properly given by $|r_{TP+} - r_{TP-}| = 2\rho$, again giving the diameter of the gyro orbit as expected. Consequently, for Type II orbits, the average of value of the two turning point radii is always equal to the gyroradius ρ . In the case where the center of the orbit coincides with the origin of the coordinate system, the value of both radial turning points is equal to ρ .

Figure 5 shows an intensity plot of the effective potential for the initial conditions corresponding to those used for Figure 4. Inspection of the figure shows that the diameter of the orbit is the same as that for Figure 3, which is expected because the magnetic field strength, particle mass and initial velocity are the same.

With knowledge of the turning points, other orbital details such as the equation of motion and the effective orbital frequency can be investigated. Beginning from the Hamiltonian, which represents the total energy of the particle, we have

$$H = \frac{P_r^2}{2m} + \frac{1}{2mr^2} \left(P_\theta - m \frac{\Omega}{2} r^2 \right)^2 = \mathcal{E}_0, \quad (15)$$

where $\mathcal{E}_0 = \frac{1}{2}mv_0^2$. Substituting for P_r in terms of \dot{r} from Equation 4 and solving for \dot{r}

we have

$$\frac{dr}{dt} = \left(\frac{2}{m} \right)^{\frac{1}{2}} \left[\left(\mathcal{E}_0 + \frac{\Omega P_\theta}{2} \right) - \frac{P_\theta^2}{2mr^2} - \frac{m\Omega^2}{8} r^2 \right]^{\frac{1}{2}}, \quad (16)$$

which can be rearranged to form

$$dt = \left(\frac{m}{2}\right)^{\frac{1}{2}} \frac{dr}{\left[\left(\frac{1}{2}mv_0^2 + \frac{\Omega P_\theta}{2}\right) - \frac{P_\theta^2}{2mr^2} - \frac{m\Omega^2}{8}r^2\right]^{\frac{1}{2}}}. \quad (17)$$

Factoring out $\left(\frac{m\Omega^2}{8r^2}\right)^{\frac{1}{2}}$ from the denominator, yields

$$dt = \frac{\left(\frac{2}{\Omega}\right)r dr}{\left[\left(\frac{8}{m\Omega^2}\right)\left(\frac{1}{2}mv_0^2 + \frac{\Omega P_\theta}{2}\right)r^2 - \left(\frac{8}{m\Omega^2}\right)\frac{P_\theta^2}{2m} - r^4\right]^{\frac{1}{2}}}. \quad (18)$$

Recognizing $\frac{4v_0^2}{\Omega^2} = 4\rho^2$, $\frac{4P_\theta}{m\Omega} = 2r_m^2$, and $\frac{4P_\theta^2}{m^2\Omega^2} = r_m^4$, Equation 18 reduces to

$$dt = \frac{\left(\frac{2}{\Omega}\right)r dr}{\left[2(r_m^2 + 2\rho^2)r^2 - r_m^4 - r^4\right]^{\frac{1}{2}}}. \quad (19)$$

Finally, making the substitution $\lambda = r^2$ and integrating, we have

$$\int dt = \frac{T}{2} = \left(\frac{1}{\Omega}\right) \int_{\lambda_{TP-}}^{\lambda_{TP+}} \frac{d\lambda}{\left[2(\lambda_m + 2\lambda_L)\lambda - \lambda_m^2 - \lambda^2\right]^{\frac{1}{2}}}, \quad (20)$$

where $\lambda_m = r_m^2$, $\lambda_L = \rho^2$, and $\lambda_{TP+,-} = r_{TP+,-}^2$. This integral represents the time required for a particle to travel from the first turning point to the second turning point, which is one-half of the orbital period, T . The solution yields

$$T = \frac{2}{\Omega} \arcsin \left(\frac{\lambda - (\lambda_m + 2\lambda_L)}{2\sqrt{\lambda_L \lambda_m + \lambda_L^2}} \right)_{\lambda_{TP-}}^{\lambda_{TP+}} = \frac{2\pi}{\Omega}. \quad (21)$$

Converting the solution to the indefinite integral back to the r coordinate, the result can be inverted to obtain an expression for the radial position of the particle as a function of time,

$$r(t) = \left[2\rho(r_m^2 + \rho^2)^{\frac{1}{2}} \sin(\Omega t + \varphi_0) + (r_m^2 + 2\rho^2) \right]^{\frac{1}{2}}, \quad (22)$$

where $\varphi_0 = \arcsin \left(\frac{r_0^2 - (r_m^2 + 2\rho^2)}{2\rho(r_m^2 + \rho^2)^{\frac{1}{2}}} \right)$ is the constant of integration. Defining

$K_1 \equiv (r_m^2 + 2\rho^2)$, $K_2 \equiv 2\rho(r_m^2 + \rho^2)^{\frac{1}{2}}$ and using the expression in Equation 22 for r , the time dependence of the azimuthal position θ can be determined with the aid of Equation 5,

$$\int d\theta = \frac{P_\theta}{m} \int \frac{dt}{K_1 + K_2 \sin(\Omega t + \varphi_0)} - \frac{\Omega}{2} t. \quad (23)$$

The solution of this integral yields

$$\theta(t) = \frac{P_0}{2m\Omega K_2 K} \left(\ln \left[\frac{1 + \frac{K_1}{K_2} \tan \left(\frac{\Omega t + \varphi_0}{2} \right) - K}{1 + \frac{K_1}{K_2} \tan \left(\frac{\Omega t + \varphi_0}{2} \right) + K} \right] - \ln \left[\frac{1 + \frac{K_1}{K_2} \tan \left(\frac{\varphi_0}{2} \right) - K}{1 + \frac{K_1}{K_2} \tan \left(\frac{\varphi_0}{2} \right) + K} \right] \right) - \frac{\Omega}{2} t + \theta_0, \quad (24)$$

where the constant $K \equiv \left(1 - \frac{K_1^2}{K_2^2} \right)^{\frac{1}{2}}$ and θ_0 is the initial angular position of the particle.

The value of $K_1/K_2 > 1$, therefore the expression for $\theta(t)$ in Equation 24 is complex, with the real part giving the angular position. Taken together, Equations 22 and 24 give a parametric representation of the particle position as a function of time.

The thick black line in Figure 6a shows a plot of an ion orbit calculated using Equations 22 and 24 for the same initial conditions as those used for Figure 1. Overlaid as a white dashed line in Figure 6a is a solution from a test particle calculation, which gives a numerical solution to Newton's 2nd Law for the particle. Figures 6b and 6c show the radial and azimuthal positions as a function of time for 3 cycles of the orbit compared to the values from the test particle calculation.

III CONCLUSIONS

Hamiltonian analysis is a useful tool in the investigation of charged particle dynamics in configurations where a one-dimensional effective potential can be constructed. We have presented the example of charged particle cyclotron motion in cylindrical coordinates with a uniform axial magnetic field. This analysis was carried out

as the first step in an investigation of the more complicated dynamics of ion motion in an experimental configuration containing a uniform background magnetic field and a radially inhomogeneous, cylindrically symmetric electric field. The treatment demonstrates the utility of the effective potential for obtaining orbital details without the explicit solution of the full equation of motion.

ACKNOWLEDGEMENTS

The author is deeply grateful for many useful discussions with R. P. Treat, G. Gatling, E. Tejero, and C. Compton. This work was supported by the Office of Naval Research.

REFERENCES

¹ D. Halliday and Robert Resnick, *Fundamentals of Physics*, 2nd edition (John Wiley & Sons, Inc., New York, 1981), Chap. 30, p.545.

² F. F. Chen, *Introduction to Plasma Physics and Controlled Fusion*, 2nd edition (Plenum Press, New York, 1983), Vol. 1, Chap. 2, p.19.

³ W. E. Amatucci, Inhomogeneous plasma flows: A review of *in situ* observations and laboratory experiments, *J. Geophys. Res.* **104**, 14481 (1999).

⁴ W. E. Amatucci, D. N. Walker, G. Ganguli, J. A. Antoniades, D. Duncan, J. H. Bowles, V. Gavriishchaka, and M. E. Koepke, *Phys. Rev. Lett.*, Plasma response to strongly sheared flow **77**, 1978 (1996).

⁵ G. Schmidt, *Physics of High Temperature Plasmas*, 1st edition (Academic Press, New York, 1966), Vol. 1, Chap. 2, p.29.

⁶ J. B. Marion, *Classical Dynamics of Particles and Systems*, 2nd edition (Harcourt Brace Jovanovich, San Diego, CA, 1970), Vol. 1, Chap. 7, p.222.

⁷ D. P. Stern, Charged particle motions in a magnetic field that reduce to motions in a potential, Am. J. Phys., **43**, 689 (1975).

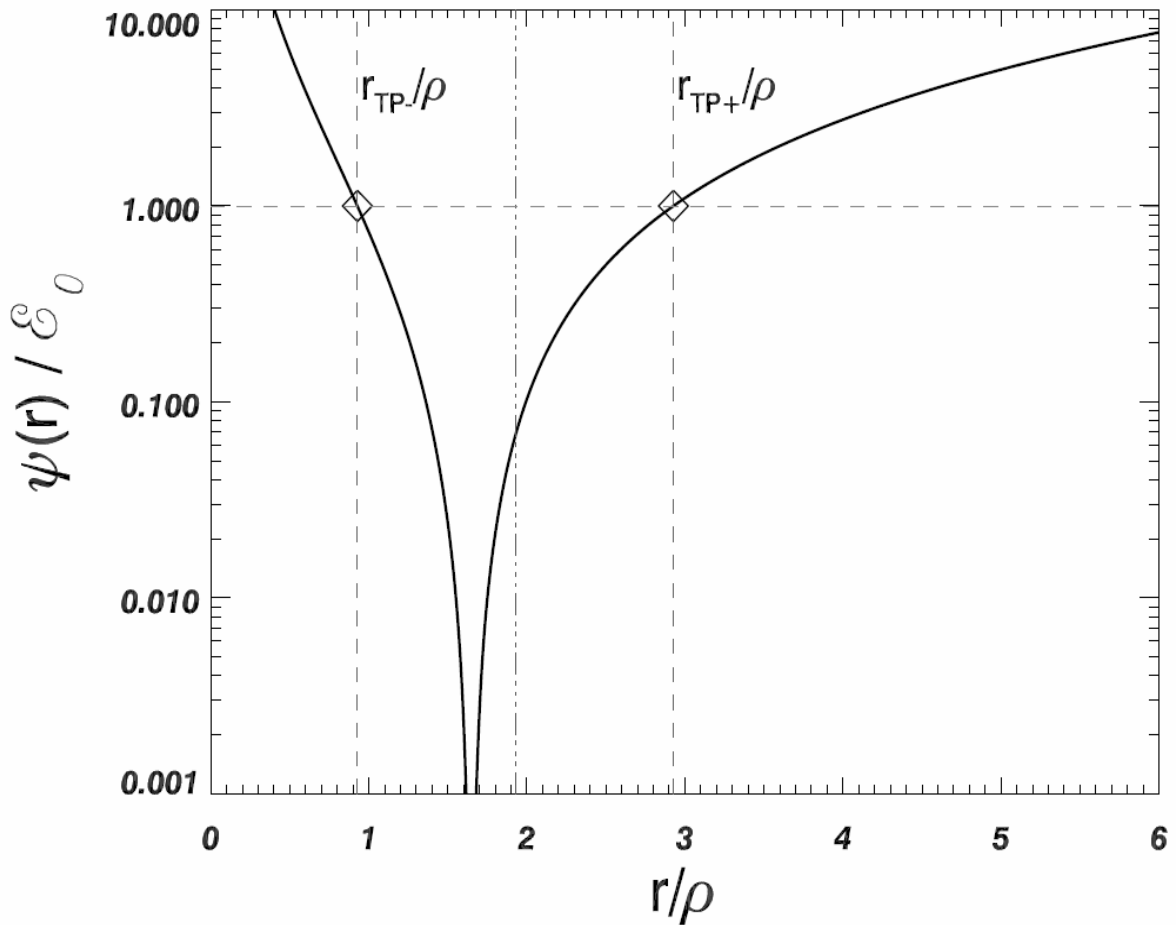


Figure 1. Effective potential $\psi(r)$ (thick black curve) for an ion in a uniform axial magnetic field. The initial ion position is 2.5ρ and the orbit is completely off axis. The horizontal dashed line at $\psi(r) = \mathcal{E}_0$ indicates the total energy of the ion. The light grey vertical dashed lines and diamond symbols indicate the inner and outer radial turning points. The dashed-dotted line indicates the radial position of the orbital guiding center. The distance between the two turning points is equal to 2ρ .

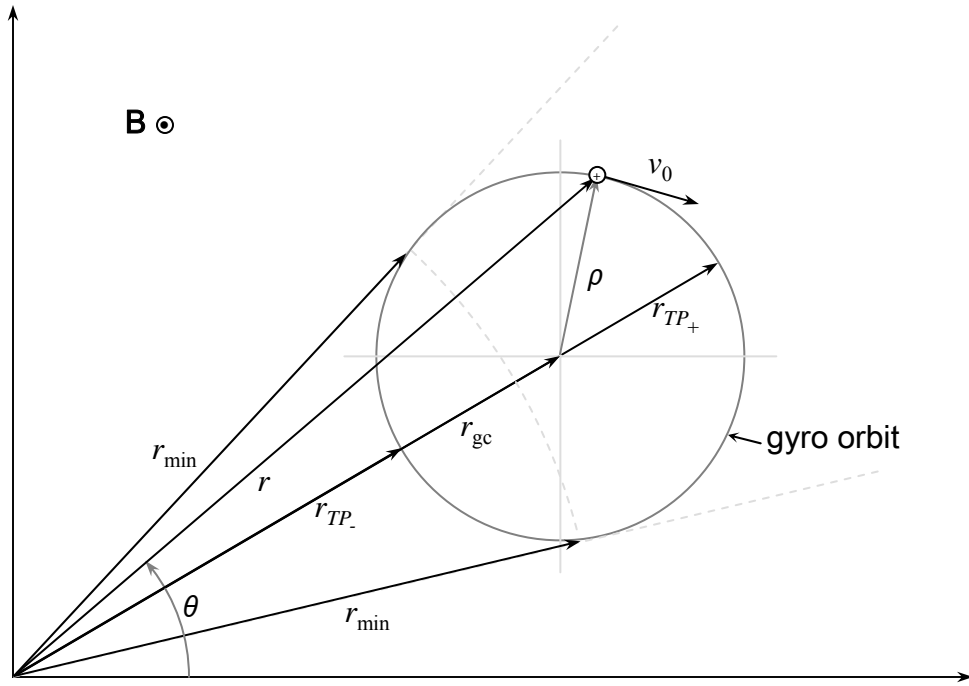


Figure 2. Schematic diagram of an off-axis ion gyro orbit in a uniform axial magnetic field. The positions of the radial and azimuthal turning points, the gyroradius, and the guiding center position are shown.

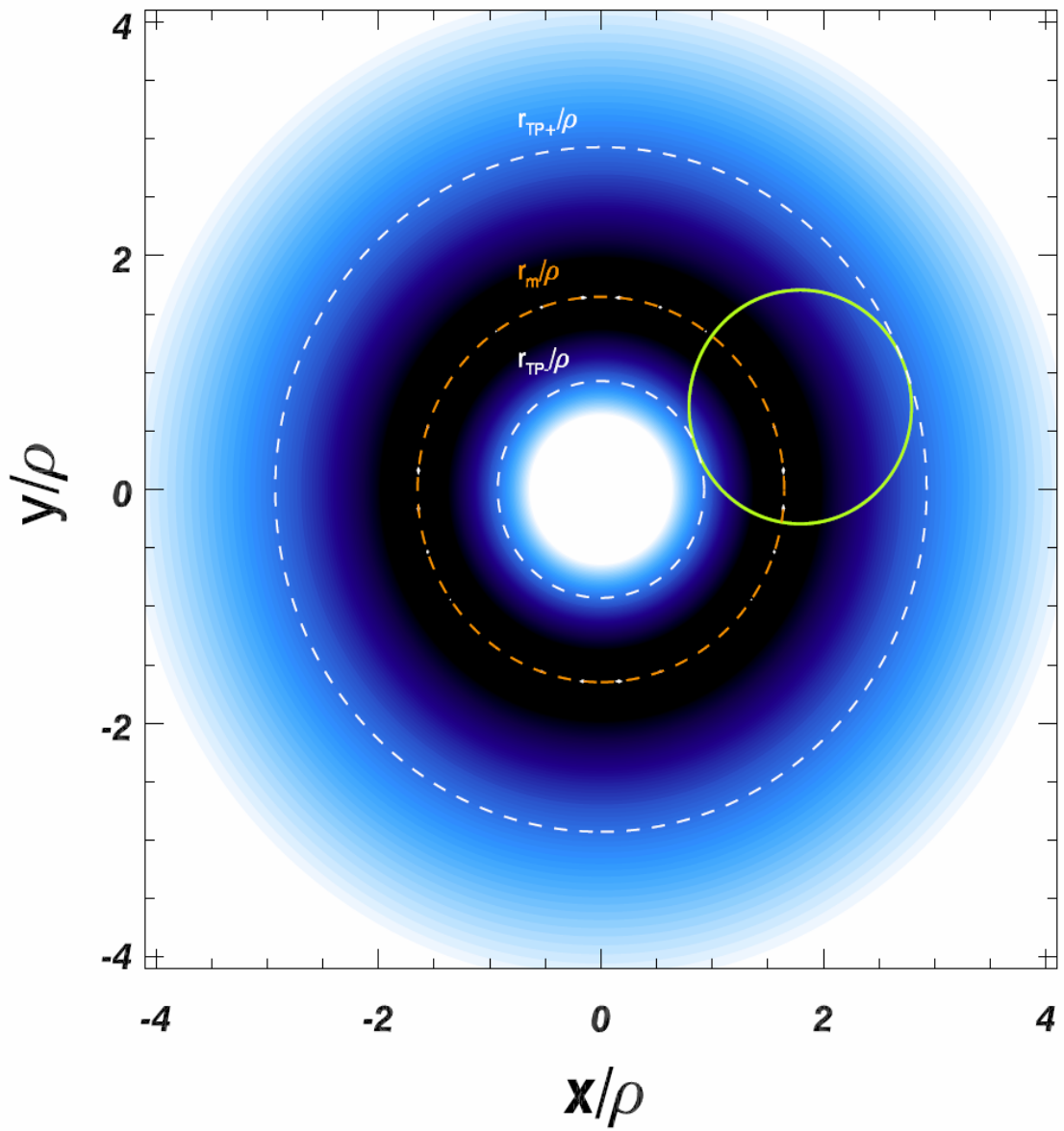


Figure 3. Intensity plot of the effective potential $\psi(r)$ in the x - y plane for an ion gyro orbit corresponding to the initial conditions for Figure 1. Black represents a value of 0, with white representing the largest magnitude of $\psi(r)$. The ion gyro orbit is indicated by the yellow line. The inner and outer turning point radii are indicated by the white dashed circles and the circle with radius equal to r_m is shown as the red dashed line.

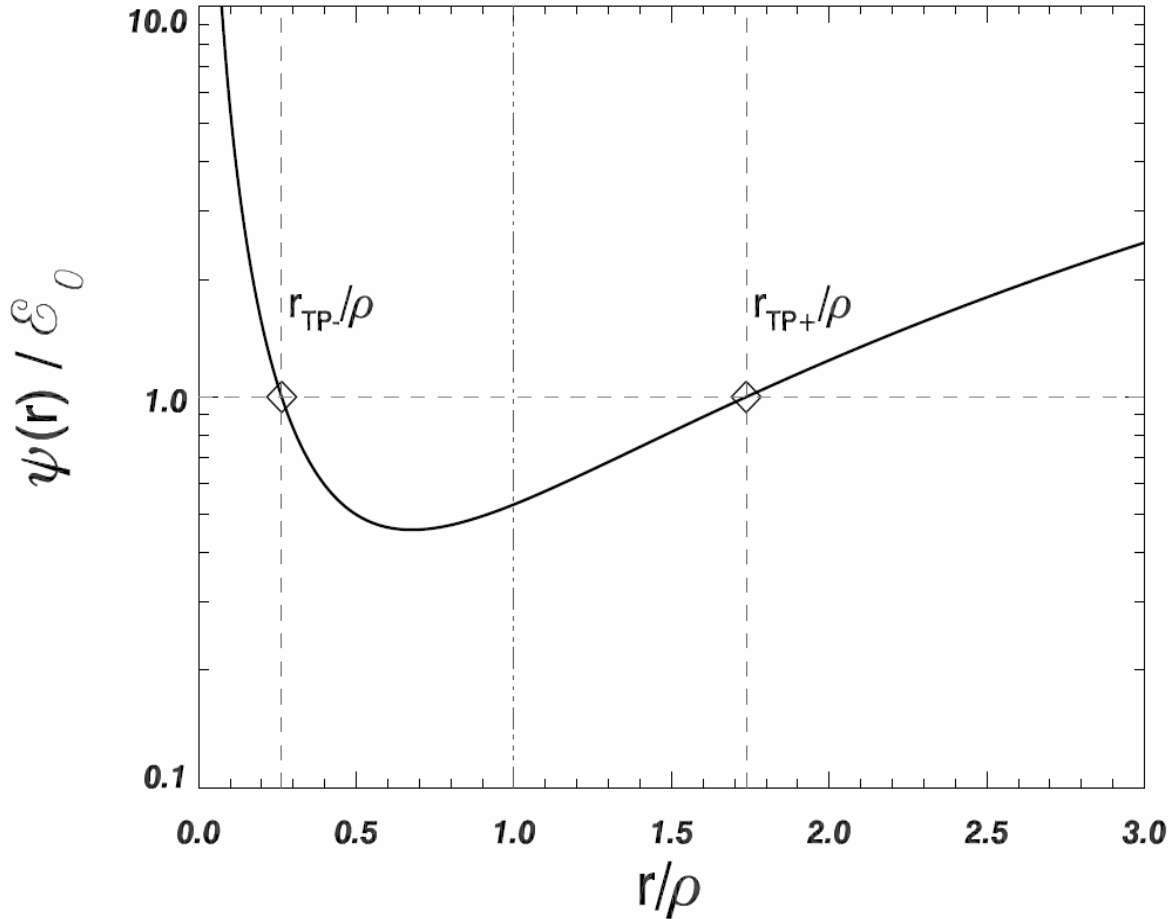


Figure 4. Effective potential $\psi(r)$ (thick black curve) for an ion in a uniform axial magnetic field. The initial ion position is 0.5ρ and the orbit encompasses the origin. The horizontal dashed line at $\psi(r) = \mathcal{E}_0$ indicates the total energy of the ion. The light grey vertical dashed lines and diamond symbols indicate the inner and outer radial turning points. The dashed-dotted line indicates the radial position of the orbital guiding center. For orbits encompassing the origin, the distance between the two turning points is equal to 2ρ since the turning points are located on opposite ‘sides’ of the origin.

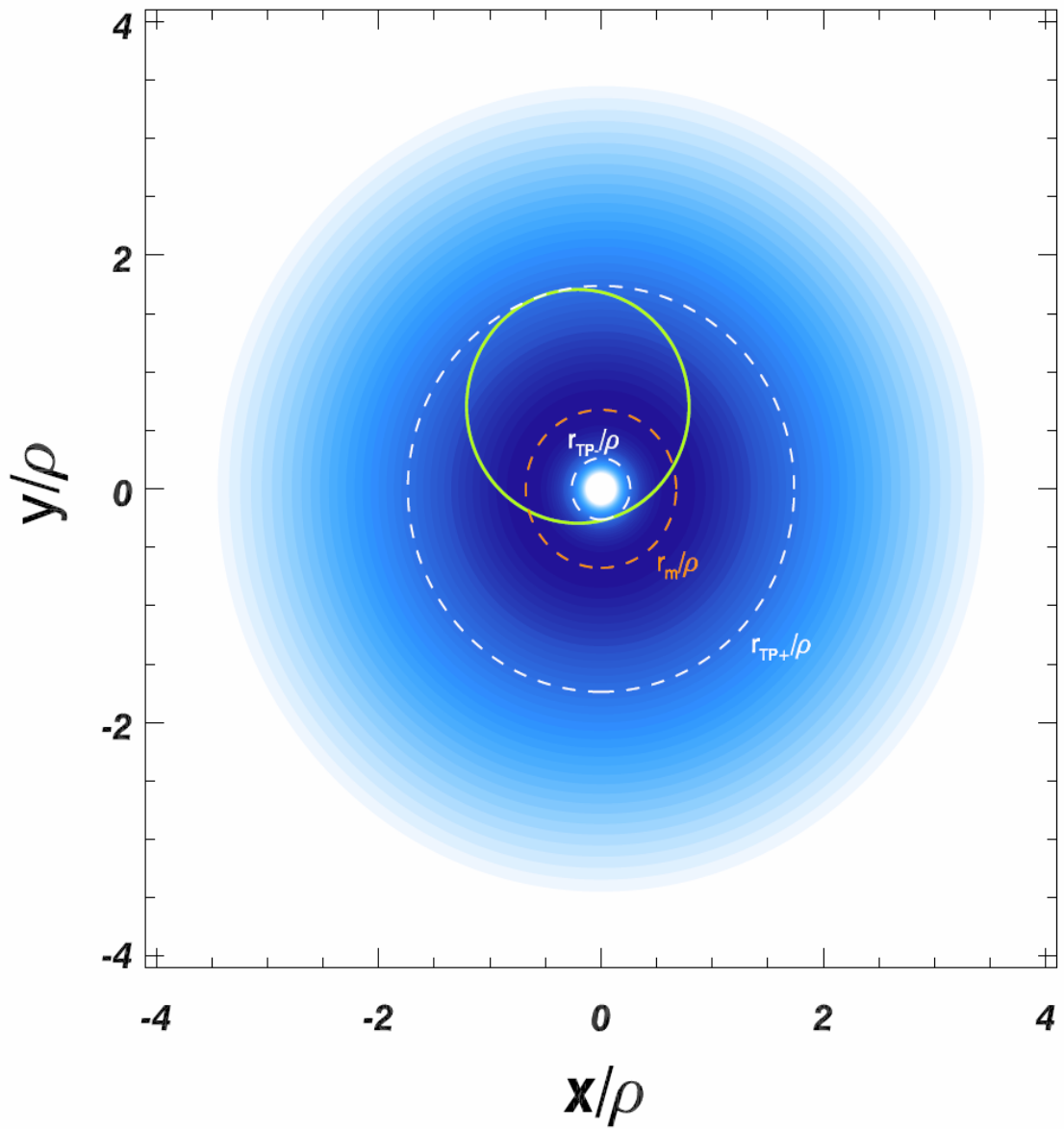


Figure 5. Intensity plot of the effective potential $\psi(r)$ in the x - y plane for an ion gyro orbit that encompasses the origin. This example corresponds to the initial conditions for Figure 4. The ion gyro orbit is indicated by the yellow line. The inner and outer turning point radii are indicated by the white dashed circles and the circle with radius equal to r_m is shown as the red dashed line. The radial turning points are seen to have an azimuthal separation of 180° .

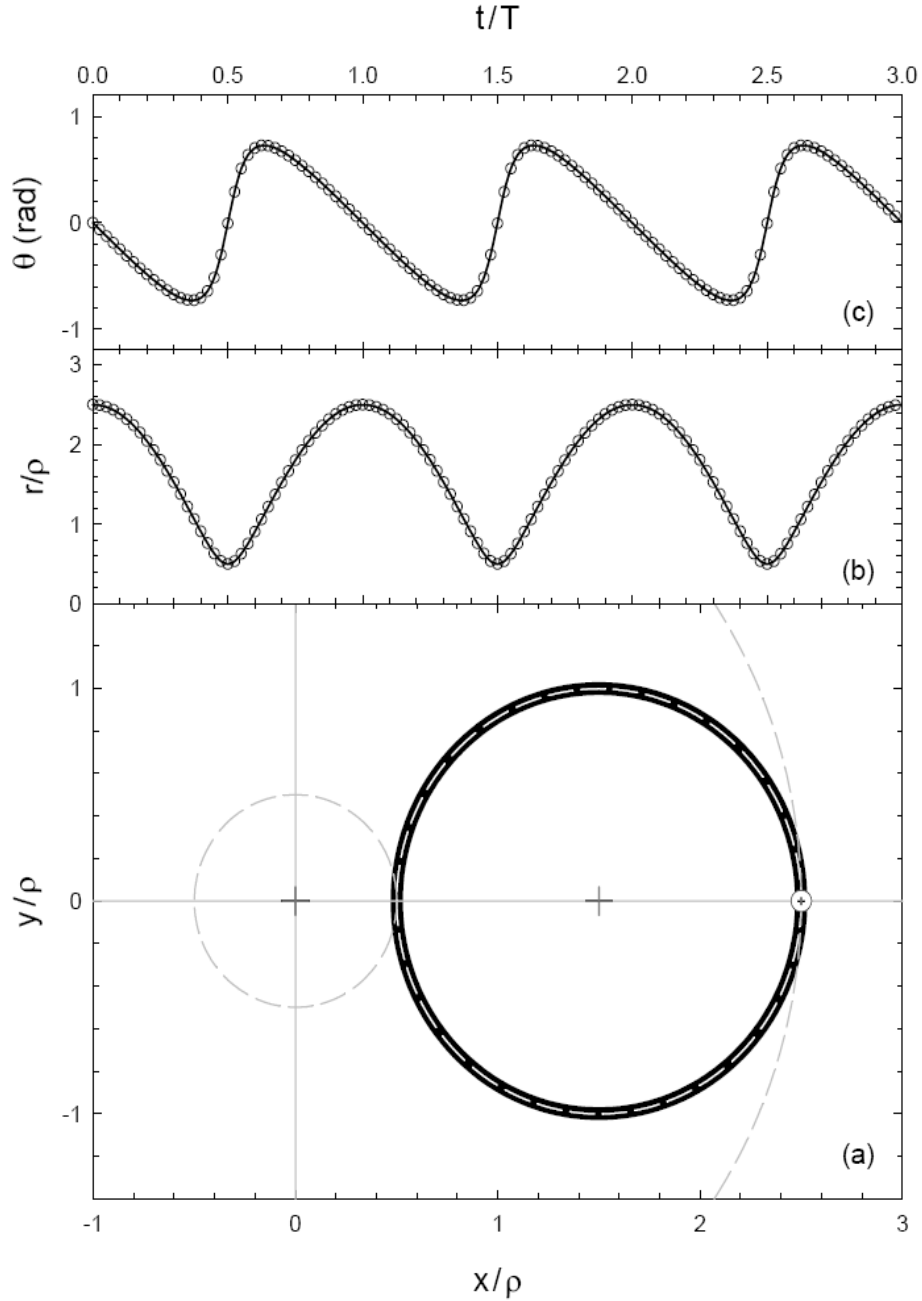


Figure 6. Comparison of the analytical solutions to the radial and azimuthal equations of motion with a numerical solution for a positively charged ion beginning from $x = 2.5\rho$ with an initial velocity in the $-y$ direction. (a) Plot of the gyro orbit. The thick black line shows the analytic results while the numerical solution is shown as the dashed white line. The inner and outer radial turning point radii are shown as the gray dashed lines. Radial (b) and azimuthal (c) components of the position as a function of time for 3 orbits. The black line shows the analytic solution while the open circles show every 50th point from the numerical solution.